Available online at www.sciencedirect.com
SCIENCE DIRECT
Journal of Power Sources 146 (2005) 622–625
JOURNAL OF POWER SOURCES
www.elsevier.com/locate/jpowsour

Synthesis and structural characterization of layered $Li[Ni_{1/3+x}Co_{1/3}Mn_{1/3-2x}Mo_x]O_2$ cathode materials by ultrasonic spray pyrolysis

Sang-Ho Park, Sung Woo Oh, Yang-Kook Sun *

Center for Information and Communication Materials, Department of Chemical Engineering, Hanyang University, Seungdong-Gu, Seoul 133-791, Republic of Korea

Available online 4 May 2005

Abstract

Molybdenum doped layered $Li[Ni_{1/3+x}Co_{1/3}Mn_{1/3-2x}Mo_x]O_2$ materials were synthesized by an ultrasonic spray pyrolysis method. A single phase of $Li[Ni_{1/3+x}Co_{1/3}Mn_{1/3-2x}Mo_x]O_2$ could be prepared in $0 \leq x \leq 0.05$ region. Structural and electrochemical properties of the $Li[Ni_{1/3+x}Co_{1/3}Mn_{1/3-2x}Mo_x]O_2$ were characterized by X-ray diffraction, Rietveld refinements and galvanostatic charge/discharge tests. The discharge capacity increased with the molybdenum doped, x in 0.01 sample is exhibited a higher discharge capacity of 175 mAh g^{-1} with a good capacity retention.

Keywords: Lithium-ion battery; Cathode materials; Molybdenum doping; Layered structure; Spray pyrolysis

1. Introduction

Lithium cobalt oxide ($LiCoO_2$) is a commercial product used in cathode materials for lithium secondary batteries. Though it has commercial applications, $LiCoO_2$ has some drawbacks such as the high cost of cobalt, toxicity and instability at high potential windows (>4.3 V) [1,2]. Therefore, many researchers have been extensively studying alternatives to $LiCoO_2$ such as $LiMO_2$ (M = Ni, Mn) layered materials. However, $LiMO_2$ layered materials have some drawbacks as well such as to the difficulty in synthesis of stoichiometric, thermal instability on $LiNiO_2$, and $LiMnO_2$ were undergone a detrimental phase transformation to a spinel phase, leading to eventual degradation of electrode performance. Although there has been much progress in optimizing $LiCoO_2$ and $LiMO_2$ layered materials, they still have some problems for more practical applications [3–6].

Recently, Yabuuchi and Ohzuku et al. reported a new layered-structure, $LiNi_{1/3}Co_{1/3}Mn_{1/3}O_2$, which was prepared by the co-precipitation method [7]. Dahn and co-workers reported that $Li[Ni_xMn_xCo_{1-2x}]O_2$ (x in 1/4 and 3/8) materials delivered a discharge capacity of 160 mAh g^{-1} when cycled between 2.5 and 4.4 V [8]. Ohzuku and Dahn et al. reported materials are different from a simple $LiNiO_2$–$LiMnO_2$–$LiCoO_2$ solid solution, because of the different oxidation states of the transition metals (Ni^{2+}, Co^{3+}, Mn^{4+}) in the simple layered $LiMO_2$ (M = Ni^{3+}, Co^{3+}, Mn^{3+}) system. Consequently, in order to increase the electro active Ni^{2+} contents, we doped $LiNi_{1/3}Co_{1/3}Mn_{1/3}O_2$ system with high valance Mo^{6+} using an ultrasonic spray pyrolysis method.

In this study, we synthesized Mo^{6+} ion doped $Li[Ni_{1/3+x}Co_{1/3}Mn_{1/3-2x}Mo_x]O_2$ ($0 \leq x \leq 0.05$) materials using MoO_3 as a starting materials. The structural and electrochemical properties of the prepared materials were characterized and the oxidation states of the transition metals are thought to be $Li[Ni^{II}_{1/3+x}Co^{III}_{1/3}Mn^{IV}_{1/3-2x}Mo^{VI}_x]O_2$.

2. Experimental

$Li[Ni_{1/3+x}Co_{1/3}Mn_{1/3-2x}Mo_x]O_2$ ($x = 0$, 0.01, 0.02, 0.05) powders were prepared as follows. Stoichiometric

* Corresponding author. Tel.: +82 2 2290 0524; fax: +82 2 2282 7329.
E-mail address: yksun@hanyang.ac.kr (Y.-K. Sun).

0378-7753/$ – see front matter © 2005 Elsevier B.V. All rights reserved.
doi:10.1016/j.jpowsour.2005.03.078

amounts of $LiNO_3$, $Ni(NO_3)\cdot 6H_2O$, $Co(NO_3)_2\cdot 6H_2O$ and $Mn(NO_3)_2\cdot 4H_2O$ were dissolved in distilled water, and MoO_3 (Merck) was dissolved in NH_4OH solution. Then, the aqueous solution was added into a continuously agitated aqueous citric acid solution. Li, Ni, Co, Mn nitric salts and Mo dissolved solution (cationic ratio of $Li:Ni:Co:Mn:Mo = 1:1/3+x:1/3:1/3-2x:x$) were dissolved in distilled water together. A small amount of lithium (6 mol%) was added for the compensation of lithium evaporation during high temperature calcination. The total metal concentration of metal nitrate was 1 M. The starting solution was atomized using an ultrasonic nebulizer with a resonant frequency of 1.7 MHz. The aerosol stream was introduced into the vertical quartz reactor heated at 500 °C. The inner diameter and length of the quartz reactor were 50 and 1200 mm, respectively. The air flow rate used as a carrier gas was 10 L min^{-1}. As-prepared powders were collected in a Teflon bag in the cylinder. The collected powders were heated in a box furnace at 900 °C for 20 h at a heating rate of 1 °C min^{-1}.

Powder X-ray diffraction (XRD, Rint-2000, Rigaku, Japan) using Cu Kα radiation was employed to identify the crystalline phase of the synthesized material. Particle morphology of the powders were observed using a scanning electron microscope (SEM, JSM 6400, JEOL, Japan). Atomic absorption spectroscopy analysis (AAS, Vario 6, AnalytikjenaAG, Germany) was employed for examination of the chemical composition. Galvanostatic charge/discharge cycling was performed with a 2032-type coin cell. For the fabrication of the positive electrode, 20 mg of $Li[Ni_{1/3+x}Co_{1/3}Mn_{1/3-2x}Mo_x]O_2$ compound was mixed with 5 mg of conductive binder (3.2 mg of TAB and 1.8 mg of graphite). The mixture was pressed on a 200 mm^2 stainless steel mesh which was used as the current collector and dried at 140 °C for 10 h in vacuum oven. The test cell was made of a cathode and a lithium metal anode (Cyprus Foote Mineral Co.) separated by porous polypropylene film (Celgard 3401). The electrolyte solution was 1 M $LiPF_6$ in a mixture of ethylene carbonate (EC) and diethyl carbonate (DEC) in a 1:1 volume ratio (Cheil Industries Inc., Korea). The cell was assembled in an argon-filled glove box. The charge/discharge measurements were carried out between 2.8 and 4.4 V Li/Li^+ at a current density of 20 mA g^{-1}.

3. Results and discussion

Fig. 1 shows the X-ray diffraction patterns of $Li[Ni_{1/3+x}Co_{1/3}Mn_{1/3-2x}Mo_x]O_2$ ($x = 0$–0.05) powders doped with various amounts of molybdenum. All samples were indexed based on a hexagonal α-$NaFeO_2$ structure with a space group of $R\bar{3}m$. No impurity-related peaks are observed from the XRD patterns with increasing Mo doping contents. Therefore, all the XRD patterns were able to be indexed as a typical layered structure without any impurity phases, which is ascribed to the homogeneous atomic scale

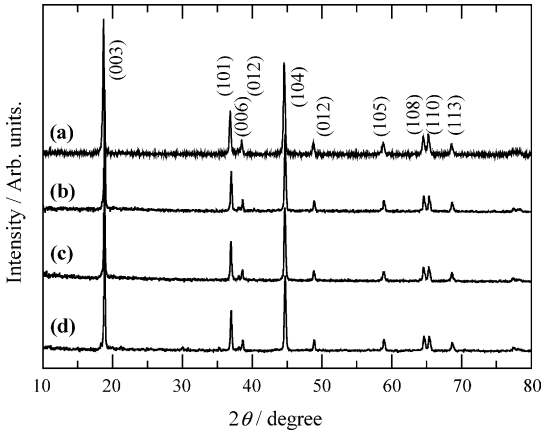

Fig. 1. X-ray diffraction patterns for $Li[Ni_{1/3+x}Co_{1/3}Mn_{1/3-2x}Mo_x]O_2$ powders prepared at various molybdenum contents: x in (a) 0, (b) 0.01, (c) 0.02, and (d) 0.05.

mixing of the precursor. The clear splitting of the reflections assigned to the Miller indices (0 0 6, 1 0 2) and (1 0 8, 1 1 0) are characteristic of the layered structure [9]. The lattice constants, a and c, c/a ratio, and I_{003}/I_{104} of the hexagonal unit cell are shown in Table 1, with the amount of Mo increased from 0 to 0.05. As the Mo contents increase, the lattice constants a and c increase from 2.85 to 2.90 Å, and 14.18 to 14.32(4) Å, respectively. The larger ionic sizes of Mo^{6+} (0.59 Å) and Ni^{2+} (0.69 Å) compared to that of Mn^{4+} (0.53 Å) might be the cause for the increased lattice parameters in the layered structure [10]. Moreover, the integrated intensity ratio of the I_{003}/I_{104} peaks decrease from 1.52 to 1.14 indicating that some cation mixing occurred in the crystal lattice between Ni^{2+} and Li^+ ion fractions, because the radii of the Ni^{2+} (0.69 Å) and Li^+ (0.76 Å) are similar. With increasing amounts of doped molybdenum, cation mixing increases. These results are concerned to increase of Ni^{2+} contents with increased contents of molybdenum.

Fig. 2 shows the scanning electron micrographs (SEM) of the $Li[Ni_{1/3+x}Co_{1/3}Mn_{1/3-2x}Mo_x]O_2$ ($x = 0.01$) powders. Fig. 2(a) shows that the precursor powders have a spherical morphology with an average particle size of about approximately 1–2 μm. On the other hand, post-calcined $Li[Ni_{1/3+x}Co_{1/3}Mn_{1/3-2x}Mo_x]O_2$ ($x = 0.01$) powders are comprised of particles of varying primary morphologies but of a consistent secondary particle size. The surface of the $Li[Ni_{1/3+x}Co_{1/3}Mn_{1/3-2x}Mo_x]O_2$ ($x = 0.01$) particles are walnut-shaped. These morphology change from precursor powder to $Li[Ni_{1/3+x}Co_{1/3}Mn_{1/3-2x}Mo_x]O_2$ ($x = 0.01$)

Table 1
Crystallographic data of the $Li[Ni_{1/3+x}Co_{1/3}Mn_{1/3-2x}Mo_x]O_2$ powders

$Li[Ni_{1/3+x}Co_{1/3}Mn_{1/3-2x}Mo_x]O_2$	a (Å)	c (Å)	c/a	I_{003}/I_{104}
$x = 0$	2.85	14.18	4.96	1.51
$x = 0.01$	2.88	14.30	4.95	1.19
$x = 0.02$	2.89	14.31	4.95	1.11
$x = 0.05$	2.90	14.32	4.94	0.95

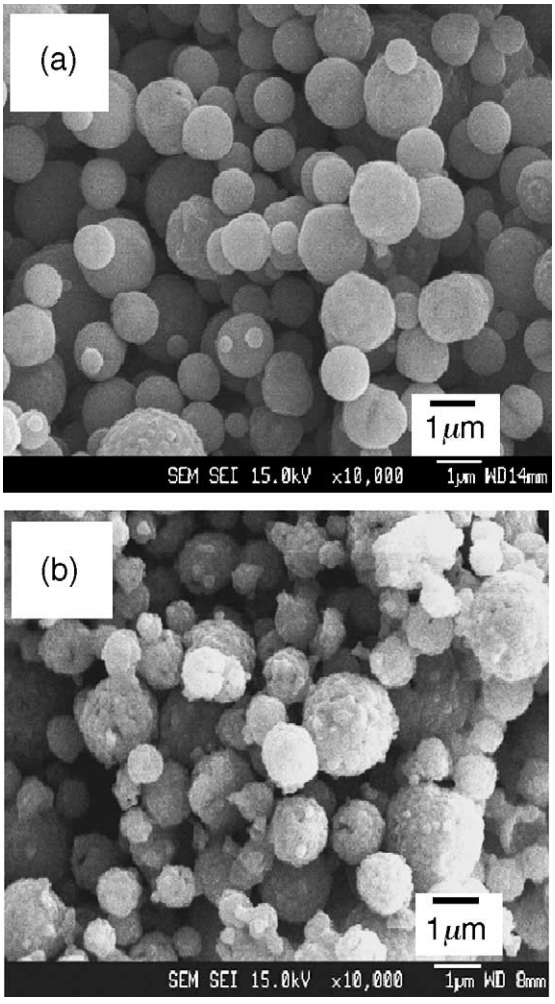

Fig. 2. Scanning electron micrographs (SEM) of (a) $Li[Ni_{1/3+x}Co_{1/3}Mn_{1/3-2x}Mo_x]O_2$ ($x = 0.01$) powder prepared at 500 °C, and (b) $Li[Ni_{1/3+x}Co_{1/3}Mn_{1/3-2x}Mo_x]O_2$ ($x = 0.01$) calcined at 900 °C.

powder are likely due to the recrystallization of precursors during the post-calcinations (900 °C) process. Detailed observations of the $Li[Ni_{1/3+x}Co_{1/3}Mn_{1/3-2x}Mo_x]O_2$ ($x = 0.01$) particle surface show that the particle surface is composed of submicron size (approximately 200 nm) primarily particles and formed secondary agglomeration.

Fig. 3(a) shows the 10th charge-discharge voltage profiles for the $Li[Ni_{1/3+x}Co_{1/3}Mn_{1/3-2x}Mo_x]O_2$ ($x = 0$, 0.01, 0.02, and 0.05) cells between 2.8 and 4.4 V at a constant current of 0.2 mA cm^{-2} (20 mA g^{-1}). All cells show a very smooth and consistent charge/discharge curves. Although not shown here, the voltage profiles for $Li/Li[Ni_{1/3+x}Co_{1/3}Mn_{1/3-2x}Mo_x]O_2$ cells did not change even after 50 cycles. This indicated that lithium ions reversible intercalated/de-intercalated into a well-ordered layered structure. Fig. 3(b) is a plot of the specific discharge capacity versus the number of cycles for $Li[Ni_{1/3+x}Co_{1/3}Mn_{1/3-2x}Mo_x]O_2$ ($x = 0$–0.05) cells at room temperature at a constant current density of 0.2 mA cm^{-2}

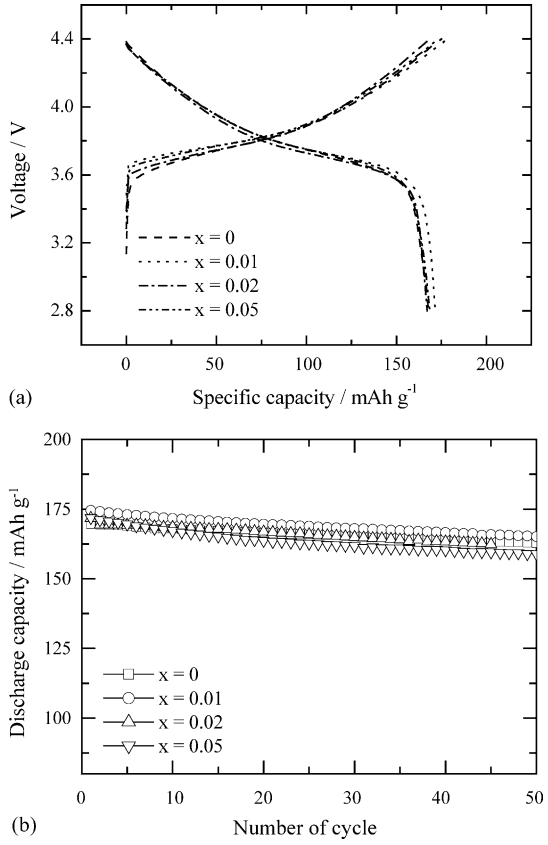

Fig. 3. (a) Charge/discharge voltage profiles, and (b) specific discharge capacity vs. number of cycles for various molybdenum contents on $Li/Li[Ni_{1/3+x}Co_{1/3}Mn_{1/3-2x}Mo_x]O_2$ cells.

(1/8C rate). The $Li/Li[Ni_{1/3}Co_{1/3}Mn_{1/3}]O_2$ cell delivered an initial discharge capacity of 169 mAh g^{-1}. However, molybdenum doped ($x = 0.01$) sample had a higher capacity of 175 mAh g^{-1} with good capacity retention. As it was suggested that if the electro-active Ni^{2+} amount increases the resulting capacity would increase, the doped sample clearly exhibited enhanced capacity during cycling, because

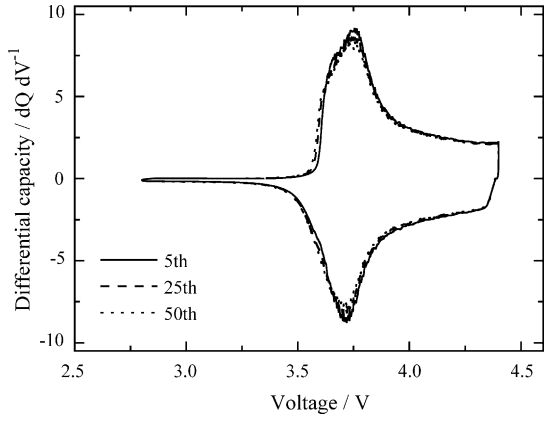

Fig. 4. Differential capacity vs. voltage for $Li/Li[Ni_{1/3+x}Co_{1/3}Mn_{1/3-2x}Mo_x]O_2$ ($x = 0.01$) cells. The cells were charged discharge between 2.8 and 4.4 V using a specific current of 0.2 mA cm^{-2}.

$Li[Ni^{II}_{1/3+x}Co^{III}_{1/3}Mn^{IV}_{1/3-2x}Mo^{VI}_{x}]O_2$ material allows Li^+ ions to be extracted more. Therefore, a partly substituted molybdenum sample could deliver a higher discharge capacity with good capacity retention.

Fig. 4 shows differential capacity versus voltage of the 5th, 25th, 50th cycles for the $Li/Li[Ni_{1/3+x}Co_{1/3}Mn_{1/3-2x}Mo_x]O_2$ ($x = 0.01$) cell. From the un-exchanged redox peak, it can be seen that structural change did not occur during the repetitive lithium extraction/insertion process. Therefore, Mo doping of $Li[Ni_{1/3}Co_{1/3}Mn_{1/3}]O_2$ is an effective means to substantially enhance capacity as well as cyclability even during higher voltage cycling.

4. Conclusion

Mo doped layered $Li[Ni_{1/3+x}Co_{1/3}Mn_{1/3-2x}Mo_x]O_2$ ($x = 0$–0.05) powder with high homogeneity and high capacity was synthesized by ultrasonic spray pyrolysis. The $Li[Ni_{1/3+x}Co_{1/3}Mn_{1/3-2x}Mo_x]O_2$ ($x = 0.01$) electrode delivered a high discharge capacity of 175 mAh g^{-1} between 2.8 and 4.4 V at a high current density of 0.2 mA cm^{-2} (20 mA g^{-1}) with good cyclability. The differential capacity versus voltage curve of the $Li[Ni_{1/3+x}Co_{1/3}Mn_{1/3-2x}Mo_x]O_2$ ($x = 0.01$) electrode showed only one redox and unchanged shape of peak, which suggest minimal structural degradation during cycling.

Acknowledgment

This research was supported by University IT Research Center Project.

References

[1] J.N. Reimers, J.R. Dahn, J. Electrochem. Soc. 139 (1992) 2091.
[2] M. Menetrier, I. Saadoune, S. Levasseur, C. Delmas, J. Mater. Chem. 9 (1999) 1135.
[3] J.R. Dahn, E.W. Fuller, M. Obrovac, U. von Sacken, Solid State Ionics 69 (1994) 265.
[4] T. Ohzuku, A. Ueda, M. Kouguchi, J. Electrochem. Soc. 142 (1995) 4033.
[5] Ammundsen, J. Paulsen, Adv. Mater. 13 (2001) 943.
[6] G. Vitins, K. West, J. Electrochem. Soc. 144 (1997) 2587.
[7] N. Yabuuchi, T. Ohzuku, J. Power Sources 119–121 (2003) 171.
[8] S. Jouanneau, K.W. Eberman, L.J. Krause, J.R. Dahn, J. Electrochem. Soc. 150 (12) (2003) 1637.
[9] A. Rougier, P. Gravereau, C. Delmas, J. Electrochem. Soc. 143 (4) (1996) 1168.
[10] R.D. Shannon, Acta Crystallogr. Sect. A: Cryst. Phys. Diffr. Theor. Gen. Crystallogr. 32 (1976) 751.